# An event-based comparison of two types of automated-recording, weighing bucket rain gauges

T. O. Keefer,[1] C. L. Unkrich,[1] J. R. Smith,[1] D. C. Goodrich,[1] M. S. Moran,[1] and J. R. Simanton[1]

Received 20 December 2006; revised 20 November 2007; accepted 24 January 2008; published 16 May 2008.

[1] A multiyear comparison of two types of automated-recording, weighing bucket rain gauges was conducted using precipitation data collected at the United States Department of Agriculture, Agricultural Research Service's Walnut Gulch Experimental Watershed in southeastern Arizona. The comparison was part of the conversion of all rain gauges on the watershed from an analog-recording, mechanical-weighing rain gauge to a data logger controlled, digital-recording, electronic-weighing rain gauge with radiotelemetry. This comparison applied to nine pairs of analog and digital rain gauges that were in coincident operation during a 5-year period, 1 January 2000 to 31 December 2004. This study found that (1) high errors in event intensities may be produced when analog charts are digitized at short time intervals; (2) dual digital rain gauges recorded precipitation equivalently; (3) for several different measures of precipitation, the analog and digital data were equivalent; and (4) implications for the rainfall-runoff model, Kinematic and Erosion Runoff model (KINEROS), showed a limited but significant effect in modeled runoff due to differences between analog and digital rain gauge input precipitation intensities. This study provided a useful analysis for long-term rain gauge networks that have recently converted, or will soon convert, from analog to digital technology. Understanding these differences and similarities will benefit interpretation of the combined long-term precipitation record and provide insights into the impacts on hydrologic modeling.

**Citation:** Keefer, T. O., C. L. Unkrich, J. R. Smith, D. C. Goodrich, M. S. Moran, and J. R. Simanton (2008), An event-based comparison of two types of automated-recording, weighing bucket rain gauges, *Water Resour. Res.*, *44*, W05S12, doi:10.1029/2006WR005841.

## 1. Introduction

[2] The United States Department of Agriculture, Agricultural Research Service, Southwest Watershed Research Center (SWRC) has operated the Walnut Gulch Experimental Watershed (WGEW) in the vicinity of Tombstone, Arizona for more than 50 years [*Renard et al.*, 2008]. The long-term precipitation record from this network has been the basis for analysis of precipitation characteristics as well as multiple simulations to study ecohydrological properties of semiarid areas [*Goodrich et al.*, 2008]. Some of the characteristics described by *Goodrich et al.* [2008] stress the seasonality of precipitation. Approximately 60% of the total annual rainfall occurs during the summer (July, August, and September) associated with the North American Monsoon (NAM). During the NAM, precipitation typically results from high-intensity air mass thunderstorms of limited spatial extent. Nearly 20% of annual precipitation falls during the winter months (January, February, and March), primarily as low-intensity rainfall, from large area, frontal systems. Runoff, generated from precipitation events, also varies seasonally with virtually all runoff generated by high-intensity storms during NAM [*Stone et al.*, 2008]. Watershed size or scale plays an important role on the dominant processes determining runoff characteristics. At smaller scales, the rates and amounts of runoff are influenced by rainfall intensity [*Osborn and Lane*, 1969]. In contrast, at larger scales, runoff is controlled by infiltration of water into the alluvial channels, referred to as channel transmission losses [*Keppel and Renard*, 1962; *Goodrich et al.*, 2004].

[3] Long-term, high-density records of precipitation on experimental watersheds are rare because they are financially and politically difficult to create and maintain. This makes sites, such as WGEW, Riesel, TX [*Harmel et al.*, 2003], Coshocton, OH [*Bonta et al.*, 2007] and Reynolds Creek, ID [*Hanson*, 2001] among others, increasingly valuable for future studies and intensifies the demand for a high degree of systematic continuity [*National Research Council*, 1991]. Further, planned networks funded by the National Science Foundation (NSF), the National Aeronautics and Space Administration (NASA) and others are designed to rely on the continuity of these data by colocating new instrumentation with existing networks like WGEW (M. S. Moran et al., Long-term data collection at USDA experimental sites for studies of ecohydrology, submitted to *Journal of Ecohydrology*, 2008). However,

[1]Southwest Watershed Research Center, Agricultural Research Service, U.S. Department of Agriculture, Tucson, Arizona, USA.


0043-1397/08/2006WR005841$09.00

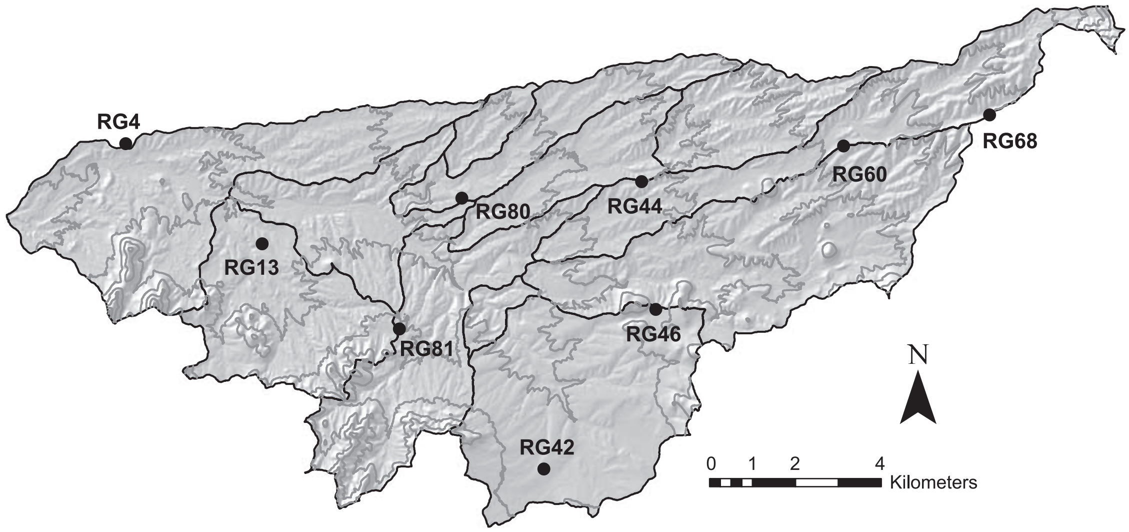


**Figure 1.** Location of the nine Walnut Gulch Experimental Watershed (WGEW) paired rain gauges used in the analysis.

technological changes in instrumentation that produce higher precision and more accurate measurements require periodic upgrades of the network. As individual instruments are replaced, continuity of location or density may be maintained, but changes in the measurement, recording or processing may affect the data record.

[4] The long-term rain gauge network at the WGEW has utilized the universal analog-recording, mechanical-weighing rain gauge. In the late 1990s at the WGEW, changes in staffing, delays in data processing and labor costs of collecting and digitizing analog charts intensified the need for digitally recorded data. The SWRC embarked on a mission to convert all rain gauges from the analog-mechanical type to a digital-electronic system driven by the availability of electronic measurements, digital recording and remote data collection. This system was designed to rely on telemetric methods for data collection and technical problem analysis.

[5] Both types of rain gauges have been described in published accounts and the complete descriptions will not be repeated here. A thorough description of the universal weighing rain gauge was reported in the Field Manual For Research In Agricultural Hydrology [*Brakensiek et al.*, 1979] and a specific description of the electronic-weighing rain gauge was given by *Hanson et al.* [2001]. The controlled comparison and analysis of the load cell rain gauge presented by *Hanson et al.* [2001] provided the basis for the choice and application of the load cell technology. A side-by-side image of both rain gauges is shown by *Goodrich et al.* [2008]. For brevity the universal analog-recording mechanical-weighing rain gauge will be referred to as "analog" and the digital-recording electronic-weighing rain gauge will be referred to as "digital."

[6] The SWRC decided that in addition to analysis similar to that described by *Hanson et al.* [2001], a 5-year record of paired measurements at multiple rain gauges would be desirable to determine the long-term field performance of the rain gauges and to allow a statistical comparison of the rain gauges. All comparisons used nine paired analog and digital rain gauges that were in coincident operation during the 5-year period from 1 January 2000 to 31 December 2004. The nine paired rain gauge sites are: 4, 13, 42, 44, 46, 60, 68, 80, and 81 (Figure 1). The analog and digital rain gauges forming each pair were located within 2 m of each other.

[7] A preliminary report on the efficacy of the rain gauges to measure and record precipitation at the event scale and the processing of data to a final database format was prepared (T. O. Keefer et al., A multi-year, multi-gage event based comparison of two types of automated-recording weighing-bucket rain gages, Southwest Watershed Research Center, Tucson, Arizona, 2006, available at http://tucson.ars.ag.gov/). In summary from that report, the analog were shown to account for 95% of all event discrepancies between the two types of gauges, where discrepancies are defined as nonmeasurement errors in the recording or processing of the data, such as unrecorded event data, erroneous dates or mechanical malfunction. The measurement, recording or processing of analog data accounted for errors in as much as 20% of the analog final data for the 5-year

**Table 1.** Number of Matched Events Per Rain Gauge Site Comparison and Season-Event Case Used in Statistical Analysis[a]

| Rain Gauge Comparison | Season-Event Case | | | | |
|---|---|---|---|---|---|
| | AY | JFM | JAS | AY5 | JAS5 |
| Digital:digital | 188 | 37 | 89 | 41 | 25 |
| Rain gauge 4 | 239 | 33 | 119 | 69 | 42 |
| Rain gauge 13 | 259 | 53 | 121 | 70 | 40 |
| Rain gauge 42 | 271 | 40 | 144 | 77 | 44 |
| Rain gauge 44 | 281 | 47 | 140 | 82 | 47 |
| Rain gauge 46 | 244 | 47 | 114 | 71 | 41 |
| Rain gauge 60 | 256 | 49 | 119 | 69 | 40 |
| Rain gauge 68 | 272 | 46 | 140 | 73 | 38 |
| Rain gauge 80 | 236 | 44 | 114 | 70 | 41 |
| Rain gauge 81 | 284 | 47 | 130 | 81 | 44 |

[a]AY: all year; JFM: January, February, and March; JAS: July, August, and September.

**Table 2a.** Means of Six Variables for Test Digital and Digital 81 for Five Season-Event Cases[a]

| | Dep, mm | | Dur, min | | Pki, mm $h^{-1}$ | | 2 pki, mm $h^{-1}$ | | 5 pki, mm $h^{-1}$ | | 30 pki, mm $h^{-1}$ | |
|---|---|---|---|---|---|---|---|---|---|---|---|---|
| Case | Test | D81 | Test | D81 | Test | D81 | Test | D81 | Test | D81 | Test | D81 |
| AY | 3.53 | 3.54 | 76.14 | 74.36 | 16.53 | 16.60 | 14.87 | 14.45 | 11.48 | 11.24 | 4.47 | 4.49 |
| JFM | 3.05 | 3.03 | 431.23 | 395.61 | 9.35 | 9.48 | 8.08 | 7.96 | 5.74 | 5.7 | 3.05 | 3.04 |
| JAS | 4.35 | 4.37 | 60.76 | 59.57 | 24.57 | 24.77 | 22.60 | 22.03 | 17.61 | 17.31 | 6.51 | 6.55 |
| AY5 | 10.88 | 10.88 | 171.00 | 171.59 | 39.2 | 38.90 | 37.54 | 36.81 | 30.56 | 29.88 | 12.81 | 12.80 |
| JAS5 | 10.41 | 10.41 | 98.66 | 96.90 | 50.38 | 49.56 | 48.17 | 46.87 | 39.01 | 38.28 | 15.47 | 15.48 |

[a]Variables are event depth (dep), duration (dur), peak intensity (pki), and peak 2-, 5-, and 30-min intensity (2 pki, 5 pki, and 30 pki, respectively). Test: test digital; D81: digital 81.

period. The measurement, recording or processing of digital data accounted for errors in approximately 1% of the final digital data for the 5-year period. It was this preliminary report and concern that the transition from old to new technology could affect time series statistics and hydrologic model output on the basis of differences in processed precipitation data that instigated this further study. The study reported here consists of (1) an analysis of errors in the process of digitizing analog charts, (2) a comparison between colocated digital rain gauges, (3) a statistical comparison of the 5-year analog and digital records, and (4) a discussion of implications for hydrologic models identifying measured precipitation variables that may impact model results.

## 2. Data and Methods

### 2.1. Analog Chart Digitizing Analysis

[8] The analysis of the digitizing of analog charts was performed to assess the accuracy of the manual digitizing process used to convert pen traces on paper rain gauge charts to digital data. The approach was to develop a more accurate digitizing method, redigitize the pen traces, and compare the two sets of data. For simplicity in retrieving the original data, and to maximize the number of points acquired from each rainfall event, 38 of the largest events from rain gauge 80 were selected, for a total of 807 individual digitized points. These points were not digitized specifically for this study, but as part of the normal data processing workflow over a period of several years. The 24-h charts (one revolution of the mechanical clock turns the chart exactly once in 24 h) were digitized using either one of two electronic tablets with manufacturer-reported accuracies of ±0.127 and ±0.254 mm (0.005, 0.01 inch) and resolution settings of 0.0254 mm (0.001 inch) for both tablets. Data were rounded to 0.254 mm (0.01 inch) for depth and the nearest whole minute for elapsed time (1 min is equivalent to 0.203 mm or 0.008 inch).

[9] To begin the redigitizing process, the pen trace for a selected rainfall event was scanned on a high-resolution flatbed digital scanner. The scanned image was then redigitized under high (16–32X) magnification in graphics software by carefully fitting a series of cubic Bézier curves through the midline of the pen trace from start to finish. The continuous trace was then rasterized to 0.0254 mm (0.001 inch) resolution for comparison to the original digitized data. The ability to obtain accurate measurements from this process was verified to within ±0.0254 mm by scanning flat metal reference shapes measured with a micrometer. However, because the thickness (approximately 0.254–0.508 mm) and irregularity of a typical ink line creates some uncertainty in locating the exact midline, the accuracy of the redigitized points is more conservatively estimated to be ±0.0508 mm (±0.002 inch). Finally it should be noted that, due to the large number of charts collected by SWRC, approximately 2500 per year, this procedure would be impractical for general use.

### 2.2. Digital-to-Digital Comparison

[10] A separate, test digital rain gauge, identical to the nine digital rain gauges used in this study, was colocated with the pair of analog and digital at site 81 for several years to investigate options of data logger programs and communications. During two periods, all of 2002 and from 24 July 2003 through 31 December 2004, the test digital rain gauge program had identical sampling and output as digital 81. These coincident measurement periods provided 188 matched precipitation events for intercomparisons of the two digital rain gauges. A precipitation event was defined as the time during which at least 0.254 mm was recorded by the rain gauge preceded and followed by a

**Table 2b.** Variances of Six Variables for Test Digital and Digital 81 for Five Season-Event Cases[a]

| | Dep, $mm^2$ | | Dur, $min^2$ | | Pki, $mm^2\ h^{-2}$ | | 2pki, $mm^2\ h^{-2}$ | | 5pki, $mm^2\ h^{-2}$ | | 30pki, $mm^2\ h^{-2}$ | |
|---|---|---|---|---|---|---|---|---|---|---|---|---|
| Case | Test | D81 | Test | D81 | Test | D81 | Test | D81 | Test | D81 | Test | D81 |
| AY | 26 | 26 | 10592 | 10729 | 500 | 466 | 450 | 419 | 292 | 287 | 47 | 46 |
| JFM | 18 | 17 | 4456 | 3655 | 290 | 328 | 185 | 206 | 63 | 63 | 15 | 15 |
| JAS | 35 | 35 | 5648 | 6176 | 822 | 751 | 751 | 694 | 494 | 490 | 82 | 81 |
| AY5 | 44 | 44 | 26912 | 27448 | 1326 | 1159 | 1155 | 1048 | 728 | 731 | 114 | 114 |
| JAS5 | 52 | 52 | 8978 | 10233 | 1374 | 1181 | 1204 | 1079 | 760 | 769 | 128 | 127 |

[a]Variables are event depth (dep), duration (dur), peak intensity (pki), and peak 2-, 5-, and 30-min intensity (2pki, 5pki, and 30pki, respectively). Test: test digital; D81: digital 81.

**Table 3a.** Means of Six Variables for Each of Nine Analog and Nine Digital for AY Case[a]

| | Dep, mm | | Dur, min | | Pki, mm h$^{-1}$ | | 2pki, mm h$^{-1}$ | | 5pki, mm h$^{-1}$ | | 30pki, mm h$^{-1}$ | |
|---|---|---|---|---|---|---|---|---|---|---|---|---|
| Site | A | D | A | D | A | D | A | D | A | D | A | D |
| 4 | 4.51 | 4.49 | 85.59 | 81.56 | 17.31 | 19.75 | 15.49 | 17.95 | 13.19 | 14.40 | 5.71 | 5.77 |
| 13 | 4.31 | 4.28 | 87.10 | 84.60 | 14.79 | 18.21 | 13.23 | 16.28 | 11.26 | 12.82 | 5.24 | 5.28 |
| 42 | 4.50 | 4.44 | 80.18 | 80.86 | 20.81 | 20.29 | 17.58 | 18.17 | 13.82 | 14.37 | 5.91 | 5.76 |
| 44 | 5.01 | 4.91 | 83.38 | 81.95 | 19.83 | 21.60 | 17.43 | 19.59 | 14.29 | 15.83 | 6.33 | 6.27 |
| 46 | 5.16 | 5.29 | 86.37 | 86.67 | 22.15 | 23.15 | 19.70 | 20.91 | 15.79 | 16.70 | 6.64 | 6.89 |
| 60 | 4.46 | 4.55 | 77.24 | 78.36 | 17.20 | 21.02 | 16.13 | 18.99 | 13.24 | 15.05 | 5.85 | 6.02 |
| 68 | 4.80 | 4.53 | 79.10 | 76.38 | 21.35 | 21.98 | 18.85 | 19.34 | 15.01 | 15.06 | 6.05 | 5.75 |
| 80 | 5.09 | 5.56 | 92.13 | 88.51 | 21.95 | 24.92 | 19.14 | 22.68 | 15.19 | 17.97 | 6.29 | 7.05 |
| 81 | 4.59 | 4.52 | 83.34 | 80.33 | 19.94 | 18.87 | 16.76 | 17.11 | 13.64 | 13.78 | 5.74 | 5.62 |

[a]Variables are event depth (dep), duration (dur), peak intensity (pki), and peak 2-, 5-, and 30-min intensity (2pki, 5pki, and 30pki, respectively). A: analog; D: digital.

hiatus of 60 min without precipitation. Events were matched between the two rain gauges by the occurrence of recorded precipitation at both gauges and the start time of an event at one rain gauge was within 60 min of the start time at the other rain gauge. The sample correlation coefficient was calculated for the matched events for the two digital rain gauges for six event variables: total depth (dep), total duration (dur), peak intensity (pki), 2-, 5-, and 30-min peak intensities (2 pki, 5 pki and 30 pki). The slope of a regression line with the $y$ intercept forced to equal zero was determined for each variable, with digital 81 as dependent variable and test digital as independent variable. Hypotheses tests on the equivalences of means and variances of these event variables were performed at the 0.05 level of confidence, with rejection of the null hypothesis when the p value was less than 0.05. All statistics were computed for five separate cases defined by a combination of three seasons and two event thresholds. As noted above and by *Goodrich et al.* [2008], the precipitation characteristics and hydroclimatology of the WGEW differ between winter and summer, and virtually all runoff at all watershed scales occurs during summer. At the smallest instrumented watershed (0.344 ha), a precipitation event threshold of 5.08 mm is required to produce runoff [*Stone et al.*, 2008]. Three seasons were defined as "all year" (AY), January, February, and March (JFM), and July, August, and September (JAS). The two event thresholds were defined as (1) all matched events and (2) all matched events for which both rain gauges recorded more than 5.07 mm. The five season-event cases were abbreviated to AY, JFM and JAS for all matched events and AY5 and JAS5 for all matched events greater than 5.07 mm. The number of matched events for each case ranged from 25 to 188 (Table 1). There were an insufficient number of events during JFM greater than 5.07 mm from which to develop meaningful statistics. Means and variances followed the expected seasonal trends, smaller event depth, lower intensity, and longer duration for JFM and greater depth, higher intensity, and shorter duration for JAS (Tables 2a and 2b).

### 2.3. Analog-to-Digital Comparison

[11] Precipitation data [*Goodrich et al.*, 2008] that were recently made available by the SWRC Data Acquisition Project [*Nichols and Anson*, 2008] were used in this analysis. Analog and digital precipitation events were matched on the basis of the same criteria as for the digital-to-digital comparison. Event data with start time differences in excess of 60 min were discarded. Event start times primarily differ for two reasons, an event not recorded by one of the pair of rain gauges or clock timing error, both of which are associated with the analog in over 95% of cases (T. O. Keefer et al., 2006). The result of this matching of events produced from 236 to 284 matched events (Table 1) for each of the nine rain gauge pairs from which the means and variances were calculated,

**Table 3b.** Variances of Six Variables for Each of Nine Analog and Nine Digital for AY Case[a]

| | Dep, mm$^2$ | | Dur, min$^2$ | | Pki, mm$^2$ h$^{-2}$ | | 2pki, mm$^2$ h$^{-2}$ | | 5pki, mm$^2$ h$^{-2}$ | | 30pki, mm$^2$ h$^{-2}$ | |
|---|---|---|---|---|---|---|---|---|---|---|---|---|
| Site | A | D | A | D | A | D | A | D | A | D | A | D |
| 4 | 32 | 30 | 8422 | 8873 | 976 | 663 | 656 | 572 | 402 | 361 | 54 | 53 |
| 13 | 28 | 30 | 8116 | 9085 | 665 | 634 | 424 | 508 | 257 | 315 | 50 | 57 |
| 42 | 41 | 41 | 9500 | 10986 | 1866 | 760 | 1015 | 672 | 502 | 442 | 92 | 86 |
| 44 | 47 | 47 | 7881 | 9032 | 1418 | 862 | 904 | 701 | 505 | 473 | 89 | 88 |
| 46 | 46 | 47 | 9451 | 11642 | 1703 | 1017 | 1142 | 874 | 648 | 556 | 97 | 103 |
| 60 | 33 | 34 | 6069 | 7113 | 910 | 728 | 758 | 627 | 396 | 405 | 61 | 66 |
| 68 | 46 | 45 | 8062 | 9117 | 1430 | 706 | 885 | 586 | 477 | 378 | 81 | 79 |
| 80 | 47 | 52 | 11324 | 10081 | 2203 | 1119 | 1491 | 970 | 754 | 662 | 95 | 107 |
| 81 | 32 | 33 | 8690 | 9774 | 1473 | 548 | 732 | 476 | 402 | 329 | 53 | 53 |

[a]Variables are event depth (dep), duration (dur), peak intensity (pki), and peak 2-, 5-, and 30-min intensity (2pki, 5pki, and 30pki, respectively). A: analog; D: digital.

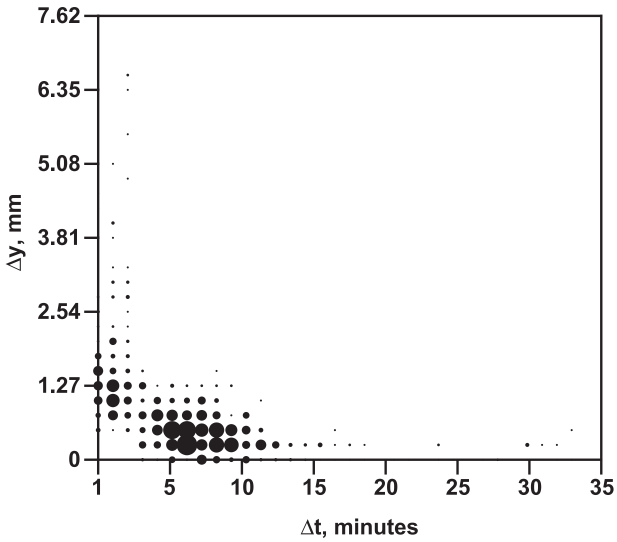


**Figure 2.** Number of times each (Δt, Δy) interval occurred in the sample of 807 points. Circle size is proportional to the number of occurrences, ranging from 1 to 29.

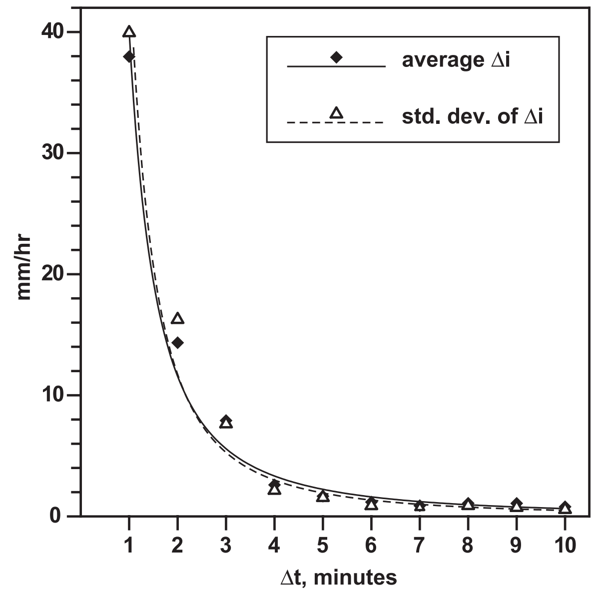


**Figure 4.** Average and standard deviation of intensity differences Δi versus digitized time interval Δt. Both curve fits are of the form $y = ax^b$, and both have correlation coefficients of 0.96.

statistics for AY are provided in Tables 3a and 3b. The matched events were used in the statistical comparison of the six event-based variables for each of five cases, identical to the digital-to-digital comparison just described. For the analog-to-digital regression, the digital was the dependent variable and the analog was the independent variable.

### 2.4. Implications for Hydrologic Models

[12] Two watersheds within the Lucky Hills study area of WGEW [*Stone et al.*, 2008], 63.106 (0.344 ha) nested within the larger 63.104 (4.53 ha), were chosen to investigate the differences in modeled runoff using analog and digital measured precipitation. Watershed model parameters were optimized by *Goodrich* [1990]. Precipitation events from the analog and digital at site 81 were selected on the basis of total rainfall depth and peak intensity. Thirty paired events were chosen from all events on the basis of total depth greater than 5.07 mm (the minimum was 6.25 mm) and with the highest peak intensities. Peak intensities ranged from 45.72 mm h$^{-1}$ to 350.52 mm h$^{-1}$ for analog and from 38.10 mm h$^{-1}$ to 152.40 mm h$^{-1}$ for digital. The minimum intensities for each gauge were within the 25 mm h$^{-1}$ to 50 mm h$^{-1}$ range used by *Syed et al.* [2003] when modeling runoff from this same watershed.

[13] The Kinematic and Erosion Runoff model (KINEROS) [*Smith et al.*, 1995] was run for each event for each analog and digital rain gauge's observed values producing results of total runoff volume, total duration, peak runoff rate and time to peak runoff rate. A coefficient of efficiency, E, introduced by *Nash and Sutcliffe* [1970] was used to assess model results. The coefficient is expressed as

$$E = 1 - \left[ \left\{ \sum_{i=1}^{30} (Q_d(i) - Q_a(i))^2 \right\} \bigg/ \left\{ \sum_{i=1}^{30} (Q_a(i) - Q_m)^2 \right\} \right] \quad (1)$$

where $Q_d$ = runoff result variable simulated from digital, $Q_a$ = runoff result variable simulated from analog, $Q_m$ =

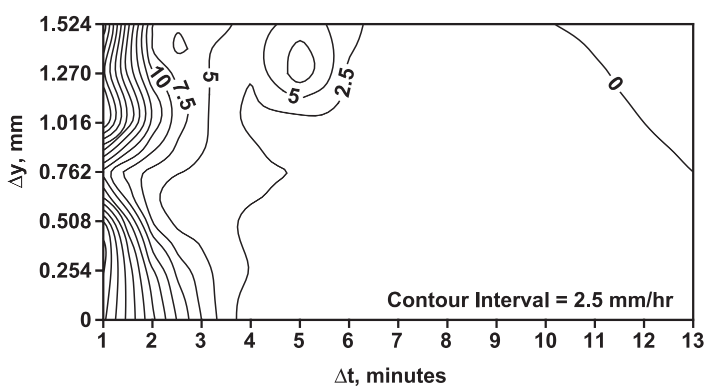


**Figure 3.** Map of average intensity differences (mm h$^{-1}$) over time and depth intervals.

**Table 4.** Hypothesis Test p Values for Comparison of Test Digital ($D_t$) and Digital 81($D_{81}$) for Six Variables and Five Season-Event Cases[a]

| Variable | AY | JFM | JAS | AY5 | JAS5 |
|---|---|---|---|---|---|
| | | $\mu_{Dt} = \mu_{D81}$ | | | |
| Dep | 0.98 | 0.99 | 0.99 | 1.00 | 1.00 |
| Dur | 0.87 | 0.94 | 0.92 | 0.99 | 0.95 |
| Pki | 0.97 | 0.97 | 0.96 | 0.97 | 0.93 |
| 2pki | 0.84 | 0.97 | 0.89 | 0.92 | 0.88 |
| 5pki | 0.89 | 0.98 | 0.93 | 0.91 | 0.92 |
| 30pki | 0.97 | 1.00 | 0.98 | 1.00 | 1.00 |
| | | $\sigma_{Dt}^2 = \sigma_{D81}^2$ | | | |
| Dep | 0.48 | 0.45 | 0.49 | 0.50 | 0.49 |
| Dur | 0.46 | 0.38 | 0.34 | 0.48 | 0.37 |
| Pki | 0.32 | 0.42 | 0.34 | 0.34 | 0.35 |
| 2pki | 0.32 | 0.43 | 0.36 | 0.38 | 0.39 |
| 5pki | 0.46 | 0.49 | 0.48 | 0.50 | 0.49 |
| 30pki | 0.48 | 0.48 | 0.48 | 0.49 | 0.49 |

[a]Equivalence of means: $\mu_{Dt} = \mu_{D81}$. Equivalence of variances: $\sigma_{Dt}^2 = \sigma_{D81}^2$. The null hypothesis of equivalence is rejected for p value less than 0.05. No null hypothesis is rejected.

mean of $Q_a$ for all events i = 1 to n, and $Q_d$ and $Q_a$ represent total runoff volume, total duration, peak runoff rate, and time to peak runoff rate from digital and analog precipitation input, respectively. If the simulation result from digital input is equivalent to that from analog input, E = 1. If the simulation result from digital input is equivalent to the mean of all results due to analog input, E = 0.

[14] Additionally, the rainstorm parameter, EI30, used in the revised universal soil loss equation (RUSLE) model [*Renard et al.*, 1997] defined as the product of storm energy and 30-min peak intensity with units of MJ $ha^{-1}$ mm $h^{-1}$ was correlated for all matched events at all rain gauge sites.

## 3. Results

### 3.1. Analog Chart Digitizing Analysis

[15] A computer program was written to compare the original digitized analog chart data against the higher-resolution data for each rainfall event. The program first aligned the two data sets by shifting the redigitized data relative to the original data both horizontally and vertically by 0.0254 mm increments until the areas trapped between the two curves are minimized. After alignment the original digitized points are matched to the nearest redigitized points, on the basis of minimal distance in any direction. The average position difference over all 807 points was 0.127 mm (0.005 inch), with a standard deviation of 0.102 mm (0.004 inch), and a median of 0.102 mm (0.004 inch).

[16] Since intensity is computed from discrete intervals of time and depth, the size of these intervals determine how much relative impact horizontal and vertical errors will have. The maximum digitized intervals of depth ($\Delta$y) and time ($\Delta$t) were 6.604 mm (0.26 inch) and 33 min, respectively, but 84% of the intervals were below 1.778 mm (0.07 inch) and 14 min (Figure 2). Mapping the average intensity difference between the original and redigitized data indicated that intensity difference is largely a function of $\Delta$t (Figure 3). The average and standard deviation of intensity difference ($\Delta$i) increase exponentially as the time interval decreases (Figure 4), suggesting that digitizing at intervals below 4 min may result in large random errors in the intensity values. In this study, 28% of the data fall into this category. This finding corroborates earlier studies such as *Brakensiek et al.* [1979, p 15], whereby the shortest time interval that should be read from a 24-h chart should be 5 min. Also, *Renard and Osborn* [1966] state that it is difficult to read rainfall amounts for intervals less than 10 min from 24-h charts.

### 3.2. Digital-to-Digital Comparison

[17] Hypothesis tests of the equivalence of means and variances for dep, dur, pki, 2 pki, 5 pki, and 30 pki were not rejected at the $\alpha = 0.05$ level for all variables and in all five cases. p values ranged from 0.84 to 1.00 for the means and 0.32 to 0.50 for the variances for all variables and all cases (Table 4). The sample correlation coefficients between the digital and the test rain gauges were greater than 0.93 for all variables in all cases (Table 5 and Figure 5). The slope of the regression lines ranged from greater than 0.94 to less than 1.03 (Table 5). On the basis of these results, it is expected that any two digital rain gauges, when similarly programmed provide statistically equivalent results. In the climate of WGEW, the data loggers are programmed to sample load cell voltage every second and average at the minute, with temporal and depth precision of 1 min and 0.254 mm.

**Table 5.** Sample Correlation Coefficients, *r*, and Regression Line Slopes (*y*-intercept forced to 0) for Digital-to-Digital Comparison of Six Variables and Five Season-Event Cases[a]

| Variable | AY *r* | AY Slope | JFM *r* | JFM Slope | JAS *r* | JAS Slope | AY5 *r* | AY5 Slope | JAS5 *r* | JAS5 Slope |
|---|---|---|---|---|---|---|---|---|---|---|
| Dep | 0.999 | 0.998 | 0.999 | 0.987 | 1.000 | 0.999 | 1.000 | 0.999 | 1.000 | 0.999 |
| Dur | 0.989 | 0.985 | 0.988 | 0.944 | 0.981 | 1.000 | 0.998 | 1.005 | 0.995 | 1.027 |
| Pki | 0.987 | 0.967 | 0.931 | 0.950 | 0.989 | 0.968 | 0.993 | 0.960 | 0.993 | 0.956 |
| 2pki | 0.993 | 0.961 | 0.978 | 0.983 | 0.994 | 0.961 | 0.996 | 0.964 | 0.996 | 0.960 |
| 5pki | 0.997 | 0.985 | 0.988 | 0.986 | 0.998 | 0.989 | 0.998 | 0.986 | 0.998 | 0.989 |
| 30pki | 0.999 | 0.998 | 0.998 | 0.993 | 1.000 | 0.999 | 1.000 | 1.000 | 1.000 | 0.999 |

[a]Correlation coefficient: *r*. Regression line slopes have *y*-intercept forced to 0.

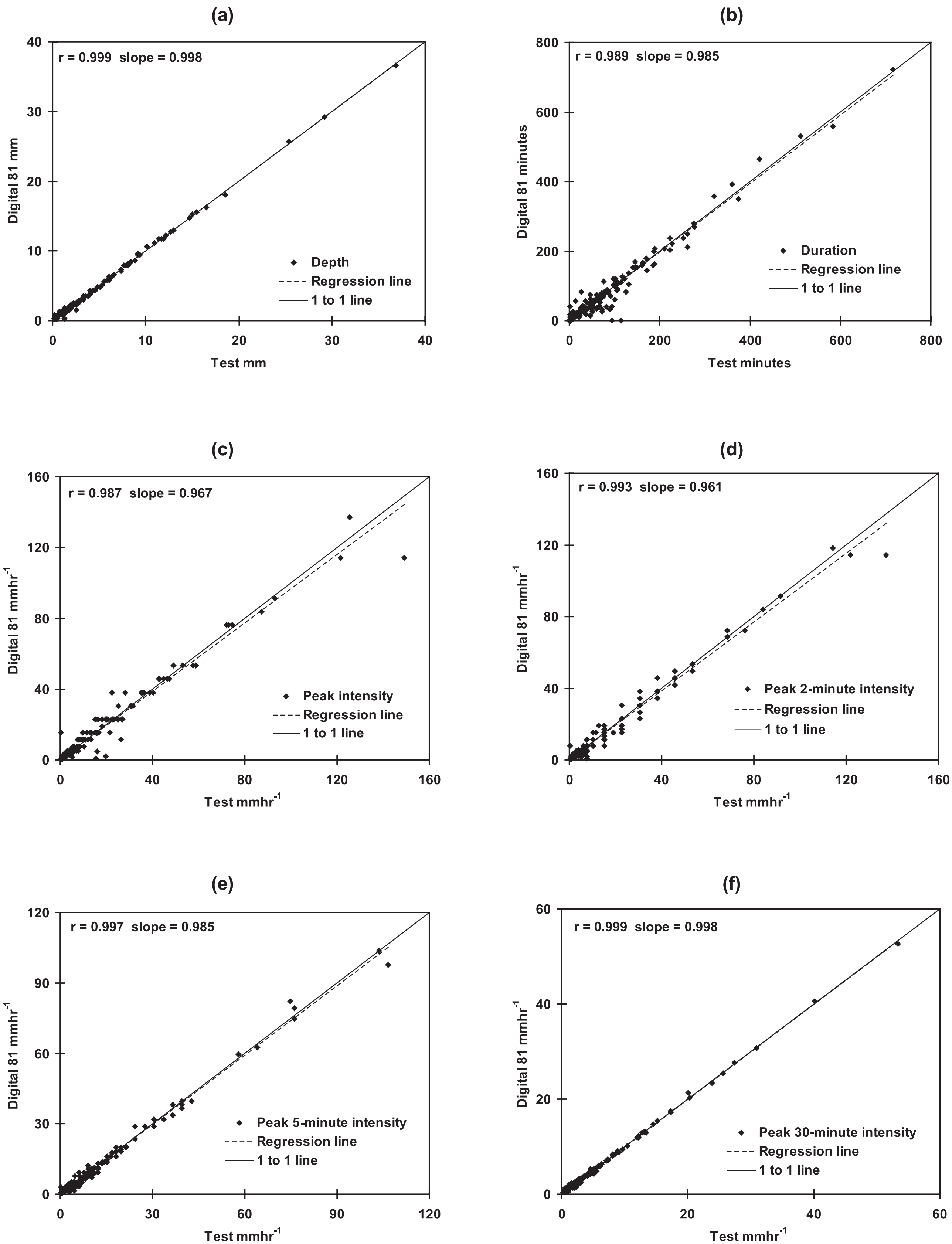


**Figure 5.** Regression line of event variables for digital-to-digital comparison, "all year" (AY) case: (a) total depth, (b) total duration, (c) peak intensity, (d) peak 2-min intensity, (e) peak 5-min intensity, and (f) peak 30-min intensity.

**Table 6a.** Hypothesis Test p Values for Analog-to-Digital Comparison at Site 81 for Six Variables and Five Season-Event Cases[a]

| Variable | Season-Event Case AY | JFM | JAS | AY5 | JAS5 |
|---|---|---|---|---|---|
| | | $\mu_A = \mu_D$ | | | |
| Dep | 0.89 | 0.95 | 0.88 | 0.90 | 0.87 |
| Dur | 0.71 | 0.81 | 0.56 | 0.92 | 0.87 |
| Pki | 0.69 | 0.77 | 0.42 | 0.16 | 0.15 |
| 2pki | 0.87 | 0.69 | 0.88 | 0.52 | 0.49 |
| 5pki | 0.93 | 0.83 | 0.99 | 0.76 | 0.80 |
| 30pki | 0.84 | 0.92 | 0.87 | 0.89 | 0.93 |

[a]Equivalence of means: $\mu_A = \mu_D$. The null hypothesis of equivalence is rejected for p value less than 0.05. Rejected null hypotheses are underlined.

### 3.3. Analog-to-Digital Comparison

[18] Hypothesis tests of event statistics and correlations of the six event variables were computed for nine pairs of analog and digital sites for five season-event cases. Results are discussed by hypothesis test on means and variances by variable, site and season-event case and similarly for correlation.

#### 3.3.1. Hypothesis Tests

[19] Hypothesis tests on the equivalence of the means were not rejected in 267 of 270 tests (nine sites, six variables, five cases). As an example, p values for site 81 ranged from a low of 0.15 for pki in JAS5 to 0.99 for 5 pki in JAS (Table 6a). The only rejections of equivalence of the mean were of mean pki for sites 44, 60 and 80 in JFM, having p values 0.033, 0.023 and 0.033, respectively. Winter storms generally had lower amounts, lower intensities and longer durations than summer storms. Breakpoints on analog charts were less well defined in winter than summer because of the low intensities. The intervals over which the analog charts were digitized on the basis of human judgment of the event breakpoints were relatively longer than the intervals detected by the digital. The three rejections occurred for those analog and digital pairs for which the JFM maximum digital pki was greater than the analog pki, by 15.24, 19.05, and 25.42 mm $h^{-1}$ for sites 44, 60, and 80, respectively. In each of these matched events, one for each site, the analog pki was equivalent to the analog 2 pki. However, if the analog pki had been determined at a 1-min time interval for the same depth, effectively doubling pki, the three hypotheses tests would not have been rejected. Analog $\Delta$i with respect to $\Delta$t at 2- and 1-min intervals had average errors and standard deviations between 10 and 40 mm $h^{-1}$ (Figure 4) which was exemplified in these three events between analog and digital.

[20] Hypotheses tests on the equivalence of variances were rejected for four variables, dur, pki, 2 pki and 5 pki, but not for dep and 30 pki. The one rejection of the equivalence of the variance of dur was for site 13 in JAS (p value of 0.047), the only rejection of all tests in all cases for this site. The variance of the digital was larger than the variance of the analog, derived primarily from differences in the frequency of event durations less than 90 min and because the analog had no events of duration less than 14 min while the digital had durations as short as 1 min (Figure 6). In comparison, the test of equivalence of variance was not rejected for dur in AY at site 13 because differences between analog and digital were less than for JAS and the analog had some durations less than 10 min (Figure 6). The two rejections of equivalence of variance for 5 pki were at sites 68 and 81 in AY (p values of 0.028 and 0.047, respectively) for which the variance of the analog was greater than variance of the digital. The equivalence of variance for 5 pki was not rejected for any other season-event case including non-

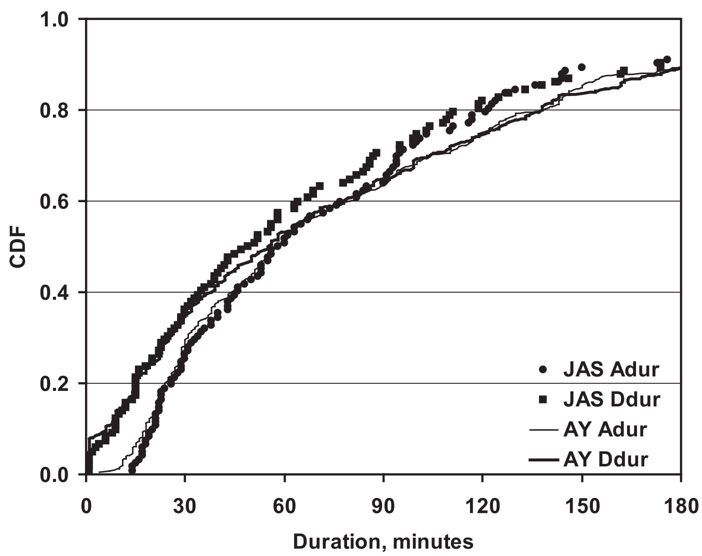


**Figure 6.** Empirical cumulative distribution function (CDF) of site 13 analog duration (Adur) and digital duration (Ddur) for July, August, and September (JAS) and AY; the equivalence of variance is rejected in JAS but not in AY. Difference in variance in JAS is due to differences in frequencies of durations less than 90 min and especially below 14 min. Duration data are truncated at 180 min.

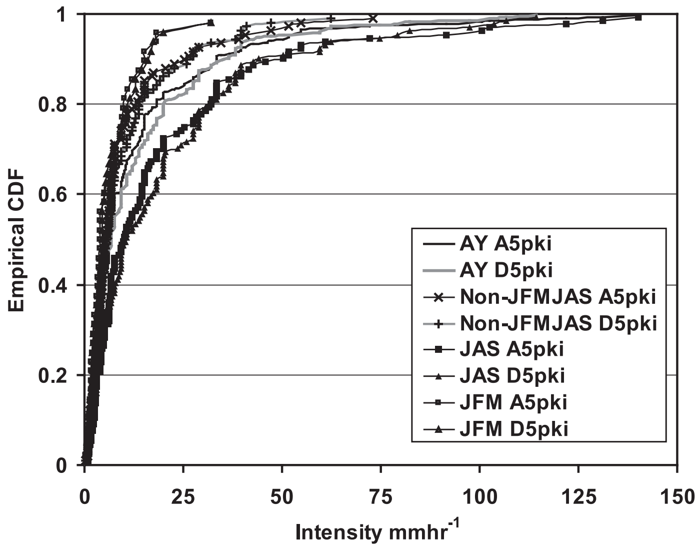


**Figure 7.** Empirical CDF of 5-min peak intensity (5pki) for analog (A) and digital (D) at site 81 for AY, January, February, and March (JFM), JAS, and non-JFMJAS; the equivalence of variance is rejected in AY but not other season-event cases.

JFMJAS, although JAS had a greater difference in analog and digital variances (Figure 7).

[21] The variables for which the equivalence of variance was predominantly rejected were pki and 2 pki, 37 and 28 rejections, respectively, of 45 tests on each variable, with p values ranging from E-16 to 0.038 for pki and from E-4 to 0.046 for 2 pki. With the exception of site 13, all sites had some rejections and the rejections occurred in all season-event cases but less so in JFM. For example, at site 81, equivalence of variance for pki and 2 pki were rejected in four season-event cases but not in JFM (Table 6b). The rejections for pki and 2 pki were due to the analog charts digitized at too fine of a time resolution, less than the 4 to 10 min recommended above. At eight of nine sites the equivalence of variance was rejected for pki in JAS and all rejections occurred when the analog variance was greater than the digital variance. At five of nine sites the equivalence of variance was rejected for pki in JFM, and four of these rejections occurred when the analog variance was less than the digital variance. Results for 2 pki were similar. These seasonal differences between the ratios of analog-to-digital variances were due to the digitized time intervals of some of the analog charts. As a chart was digitized for JAS events, an artificially high intensity digitized over a short interval was followed by a lower intensity, but only the artificially high values were reported in the pki and tended to increase the variance of pki. Conversely, as a chart was digitized for JFM events, artificially low intensities resulted from smaller depths digitized over relatively longer intervals that reduced the range and thus the variance of pki. As the time interval of intensities increased the ratio of analog-to-digital variances approached 1.0 at all sites and for both JFM and JAS (Figure 8).

**Table 6b.** Hypothesis Test p Values for Analog-to-Digital Comparison at Site 81 for Six Variables and Five Season-Event Cases[a]

| | Season-Event Case | | | | |
|---|---|---|---|---|---|
| Variable | AY | JFM | JAS | AY5 | JAS5 |
| | | $\sigma_A^2 = \sigma_D^2$ | | | |
| Dep | 0.48 | 0.49 | 0.48 | 0.46 | 0.49 |
| Dur | 0.16 | 0.36 | 0.24 | 0.26 | 0.25 |
| Pki | E-16 | 0.26 | E-10 | E-08 | E-06 |
| 2pki | E-04 | 0.37 | E-03 | E-03 | 0.01 |
| 5pki | 0.05 | 0.44 | 0.10 | 0.09 | 0.12 |
| 30pki | 0.50 | 0.42 | 0.45 | 0.47 | 0.46 |

[a]Equivalence of variances: $\sigma_A^2 = \sigma_D^2$. The null hypothesis of equivalence is rejected for p value less than 0.05. Rejected null hypotheses are underlined.

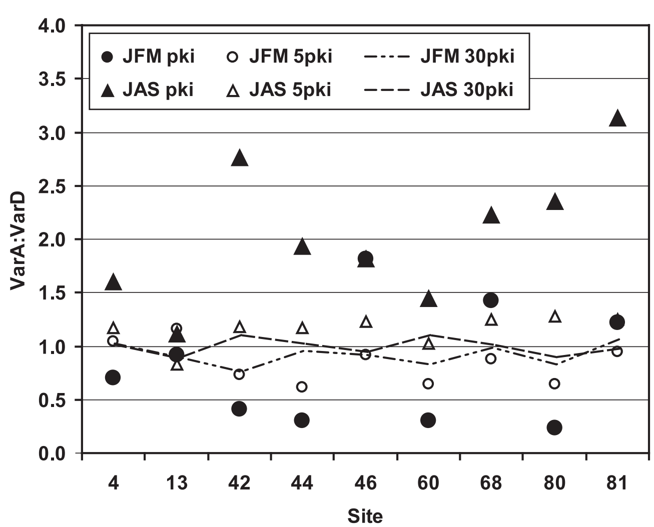


**Figure 8.** Analog-to-digital ratio of the variances of pki, 5pki, and 30pki for nine rain gauge sites for JAS and JFM.

**Table 7a.** Analog-to-Digital Comparison for the AY Case of Nine Sites and Six Variables and EI30 Sample Correlation Coefficient

| | Comparison Site | | | | | | | | |
|---|---|---|---|---|---|---|---|---|---|
| Variable | 4 | 13 | 42 | 44 | 46 | 60 | 68 | 80 | 81 |
| Dep | 0.998 | 0.998 | 0.998 | 0.998 | 0.997 | 0.998 | 0.997 | 0.996 | 0.997 |
| Dur | 0.974 | 0.973 | 0.982 | 0.971 | 0.970 | 0.969 | 0.962 | 0.960 | 0.963 |
| Pki | 0.929 | 0.932 | 0.923 | 0.901 | 0.933 | 0.922 | 0.909 | 0.910 | 0.899 |
| 2pki | 0.960 | 0.964 | 0.953 | 0.945 | 0.970 | 0.942 | 0.956 | 0.941 | 0.960 |
| 5pki | 0.984 | 0.984 | 0.987 | 0.981 | 0.983 | 0.981 | 0.981 | 0.975 | 0.979 |
| 30pki | 0.998 | 0.998 | 0.996 | 0.998 | 0.996 | 0.997 | 0.997 | 0.994 | 0.997 |
| EI30 | 0.999 | 1.00 | 0.995 | 0.999 | 0.996 | 0.998 | 0.999 | 0.991 | 0.998 |

#### 3.3.2. Correlation

[22] The correlation between analog and digital variables was >0.99 for dep, >0.93 for dur, >0.96 for 5 pki and >0.97 for 30 pki for all sites and all season-event cases, listed for AY in Table 7a. For pki and 2 pki, for which most of the tests of equivalence of means and variances were rejected, the correlation ranged from 0.81 to 0.95 and 0.87 to 0.98, respectively. The variable with the overall minimum correlation, pki, also had the minimum correlation at all nine sites and for all five season-event cases. Although correlation was generally high, the slope of the regression line showed greater differences. In general dep, dur, 5 pki and 30 pki had slopes near 1.00, between 0.93 and 1.10 for dep to between 0.88 and 1.22 for 5 pki, presented for AY in Table 7b. All of these maximum and minimum slopes occurred in JFM, indicating better one-to-one correspondence between analog and digital in JAS and AY. For pki and 2 pki, the greatest slopes also occurred in JFM, 1.72 and 1.58, respectively, associated with the rejection of equivalence of mean pki at sites 44, 60 and 80. In JFM the digital pki and 2 pki were greater than the analog because of lower intensities digitized from some analog charts for winter storms. However, the minimum slopes for pki and 2 pki occurred in JAS, 0.60 and 0.80 respectively. Errors introduced by digitizing high-intensity and short-duration summer storms from analog charts, especially at intervals less than the 4-min minimum, caused the artificially high pki and 2 pki.

[23] Using site 81 as an example (Figure 9) correlation of pki was 0.926 for JAS5, and correlations for other variables were greater than 0.97 (Table 8). Regression line slopes for pki were lower than other variables (Table 8) and were lowest in JAS5, AY5, JAS and AY. Similar results are found for 2 pki, albeit higher slopes than pki. These low slopes indicate higher peak intensities for analog than digital. The low slopes of pki, and less so for 2 pki, are a result of errors in intensity introduced in the digitizing process of the analog charts. The time interval for calculation of each of these intensities is less than the 4-min minimum interval described above. All 5 pki and 30 pki have correlation of 0.97 or greater and slopes between 0.91 and 1.10 (Tables 7a, 7b, and 8). For intensities at longer intervals, 30 pki, the analog and digital have been shown to be equivalent in the previous section. It is the higher peak intensities, specifically those identified for pki in the JAS5 case, which will have implications for hydrologic models using intensity as a driving variable.

### 3.4. Implications for Hydrologic Models

[24] One of many uses of precipitation data collected at the WGEW is to parameterize or provide input to hydrologic simulation models. These models require accurate data at a variety of timescales and in a variety of engineering units. RUSLE and KINEROS are two such models. Each of these models requires an aspect of measured precipitation to develop needed parameters or as model input. The preceding sections have highlighted some of the similarities and discrepancies between precipitation measured by the analog and digital rain gauges. In this section, the effects of those similarities and differences will be briefly considered in light of the needs of these models.

#### 3.4.1. RUSLE

[25] The EI30 parameter of RUSLE is used to represent the physical impact of rainfall energy on the erosion process. *Renard and Ferreira* [1993] performed sensitivity analysis for EI30 on soil loss, by changing EI30 inputs from various midwestern and western U.S. locations but applied to the same field conditions of soil, slope, area, and management practice. They found that changing from

**Table 7b.** Analog-to-Digital Comparison for the AY Case of Nine Sites and Six Variables and EI30 Regression Line Slope

| | Comparison Site | | | | | | | | |
|---|---|---|---|---|---|---|---|---|---|
| Variable | 4 | 13 | 42 | 44 | 46 | 60 | 68 | 80 | 81 |
| Dep | 0.983 | 1.010 | 0.992 | 0.989 | 1.018 | 1.020 | 0.971 | 1.058 | 0.993 |
| Dur | 0.967 | 0.989 | 1.029 | 1.000 | 1.032 | 1.016 | 0.983 | 0.975 | 0.981 |
| Pki | 0.844 | 0.974 | 0.660 | 0.772 | 0.785 | 0.909 | 0.722 | 0.733 | 0.626 |
| 2pki | 0.960 | 1.095 | 0.829 | 0.896 | 0.899 | 0.927 | 0.841 | 0.842 | 0.836 |
| 5pki | 0.977 | 1.099 | 0.955 | 0.991 | 0.948 | 1.031 | 0.910 | 0.975 | 0.920 |
| 30pki | 0.999 | 1.041 | 0.964 | 0.993 | 1.028 | 1.034 | 0.970 | 1.072 | 0.989 |
| EI30 | 0.979 | 1.097 | 0.880 | 0.977 | 1.082 | 1.083 | 0.949 | 1.113 | 1.023 |

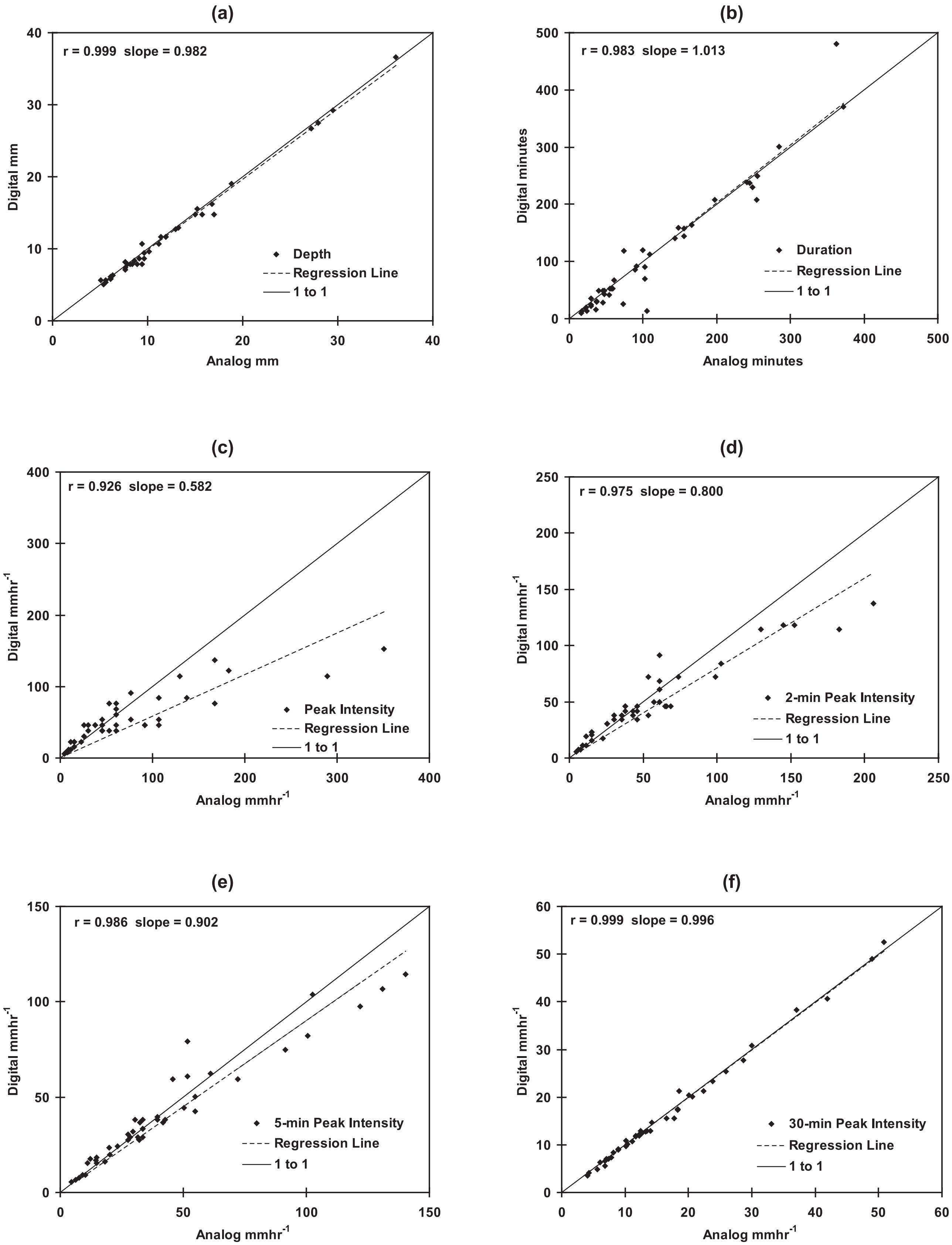


**Figure 9.** Regression line for each of six event variables for analog-to-digital comparison site 81 (a) total depth, (b) total duration, (c) peak intensity, (d) 2-min peak intensity, (e) 5-min peak intensity, and (f) 30-min peak intensity for JAS5.

**Table 8.** Sample Correlation Coefficients, *r*, and Regression Line Slopes for Analog-to-Digital Comparison at Site 81 for Six Variables and Five Season-Event Cases[a]

| | Season-Event Case | | | | | | | | | |
|---|---|---|---|---|---|---|---|---|---|---|
| | AY | | JFM | | JAS | | AY5 | | JAS5 | |
| Variable | *r* | Slope | *r* | Slope | *r* | Slope | *r* | Slope | *r* | Slope |
| Dep | 0.997 | 0.993 | 0.997 | 0.988 | 0.996 | 0.984 | 0.999 | 0.993 | 0.999 | 0.982 |
| Dur | 0.963 | 0.981 | 0.935 | 0.936 | 0.953 | 0.950 | 0.993 | 1.031 | 0.983 | 1.013 |
| Pki | 0.899 | 0.626 | 0.919 | 0.894 | 0.907 | 0.597 | 0.928 | 0.600 | 0.926 | 0.582 |
| 2pki | 0.960 | 0.836 | 0.963 | 1.032 | 0.964 | 0.817 | 0.976 | 0.810 | 0.975 | 0.800 |
| 5pki | 0.979 | 0.920 | 0.970 | 1.004 | 0.981 | 0.918 | 0.986 | 0.901 | 0.986 | 0.902 |
| 30pki | 0.997 | 0.989 | 0.995 | 0.970 | 0.998 | 0.994 | 0.999 | 0.991 | 0.999 | 0.996 |

[a]Sample correlation coefficient: *r*.

a site, Chicago IL, to other sites within the same climatological area (e.g., upper midwestern United States) of low winter EI30 and high summer EI30, but slightly different annual distributions of EI30, accounted for small changes (<3%) in soil loss. Changing to a climate area with a more skewed distribution of EI30, Denver CO, had only a small impact, about 5%, on soil loss prediction. However, the change to a climate with peak EI30 in winter and lower-intensity precipitation (San Francisco, California) had a significant effect on predicted soil loss with a difference of about 50%. The high degree of correlation between EI30, calculated from precipitation intensity measured by the analog and digital rain gauges (Tables 7a, 7b and Figure 10), suggests that there should be no measurable difference in model results when using data from one or the other gauge.

### 3.4.2. KINEROS

[26] KINEROS makes use of the measured precipitation time-depth pairs to construct precipitation time-intensity pairs. Intensities that are artificially high will contribute to an increase in generated runoff and erosion. As mentioned earlier, on the WGEW at least 5.08 mm of precipitation is required to generate runoff at watershed areas of 0.344 ha. Precipitation dominates the rainfall-runoff mechanism at these scales. However, at larger scales, where hillslope runoff contributes to channel runoff, channel transmission losses become one of the dominant factors [*Goodrich et al.*, 1997].

[27] The differences in precipitation peak intensity and within-storm intensity patterns will impact simulated runoff rates. It is hypothesized that at small watershed scales, where precipitation dominates the runoff process, that the differences in measured precipitation intensity between the analog and digital will cause differences in simulated runoff. Alternatively, at a larger scale, the impact of the difference in analog and digital precipitation will be damped or mitigated by increasing infiltration losses in the influent environment of the WGEW. The Lucky Hills watersheds have been studied and modeled using different versions of KINEROS for two decades [*Goodrich*, 1990]. *Faures et al.* [1995] studied the effects of a varying number of rain gauges on model performance on these small semiarid watersheds. Correlations of these event depths and peak intensities are shown in Figure 11, along with 2-min, 5-min, and 30-min peak intensities. Whereas the total depths were nearly equivalent, the analog storm peak intensity and 2-min and 5-min peak intensities were greater than the digital. For the longer-interval peak intensities the

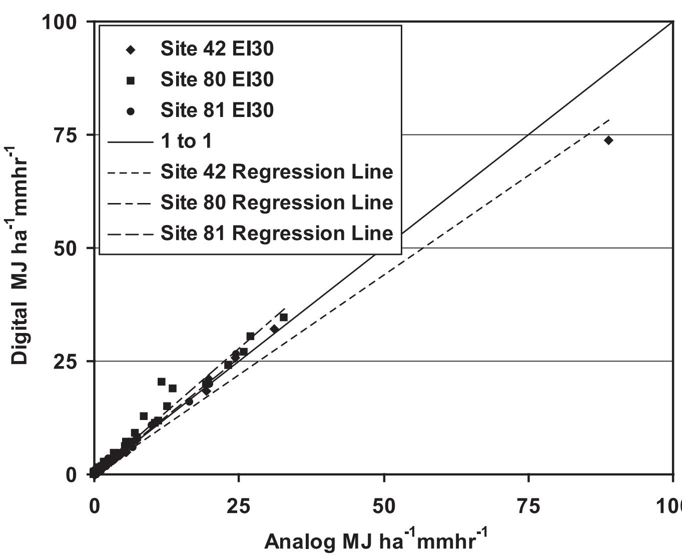


**Figure 10.** Regression line of EI30 for analog-to-digital comparison for sites 42, 80, and 81.

digital and analog were equivalent. It is this difference in peak intensity at less than 5-min intervals that should cause differences in simulated runoff.

[28] For the four summary results for each of the watershed simulations, the total volume and time to peak are simulated equally well for both watersheds, with E of 0.98 for volume and about 0.94 for time to peak rate (Table 9). E of duration at 63.104 (0.89) is 150% greater than at 63.106, and E of peak rate at 63.104 (0.95) is 60% greater than at 63.106. Thus the model simulation of 63.106 is significantly affected by the difference in precipitation input, whereas at the order-of-magnitude larger scale, 63.104, the precipitation inputs were damped by routing and channel effects, as anticipated.

[29] Simulated analog and digital volumes at both 63.106 and 63.104 were nearly equivalent (Figure 12). However, there is considerable difference in peak runoff rates due to analog and digital rainfall inputs, especially for 63.106. Watershed scale plays a role in ameliorating the effects of differences in measured rates. But at the small scales for which precipitation controls runoff production, these measured precipitation differences as hypothesized will have significant impact on model results.

## 4. Discussion and Conclusions

[30] The results of this study have shown that large errors in precipitation event intensity are a product of analog charts digitized at a time resolution below 5 min. Precipitation events measured at two colocated digital rain gauges did not differ significantly from each other. This suggested that identically designed and programmed digital rain gauges will produce statistically equivalent results of measured precipitation. Using matched events for each pair of rain gauges, the analog and digital were equivalent for several different measures of precipitation including the means of event depth, duration, 2-min, 5-min, and 30-min peak intensities. At three of nine sites in the hydrologically inactive winter season, the means of analog and digital peak intensities were not equivalent, but this was a result of a single event at each site with lower analog than digital peak intensity. The variances of depth and 30-min peak intensity were equivalent as were the variances of duration and 5-min peak intensity for the majority of sites and season-event cases. However, for the variances of event peak intensity and 2-min peak intensity, the analog and digital rain gauges differed significantly. These differences were due to errors produced from the analog charts digitized at a time resolution below 5 min. The differences were realized in the peak intensities of summer precipitation events, for which analog peak intensities for some events were much greater than digital peak intensities.

[31] Using the results of the statistical analysis, the impacts of similarities and differences in various measures of precipitation were discussed in terms of effect on two

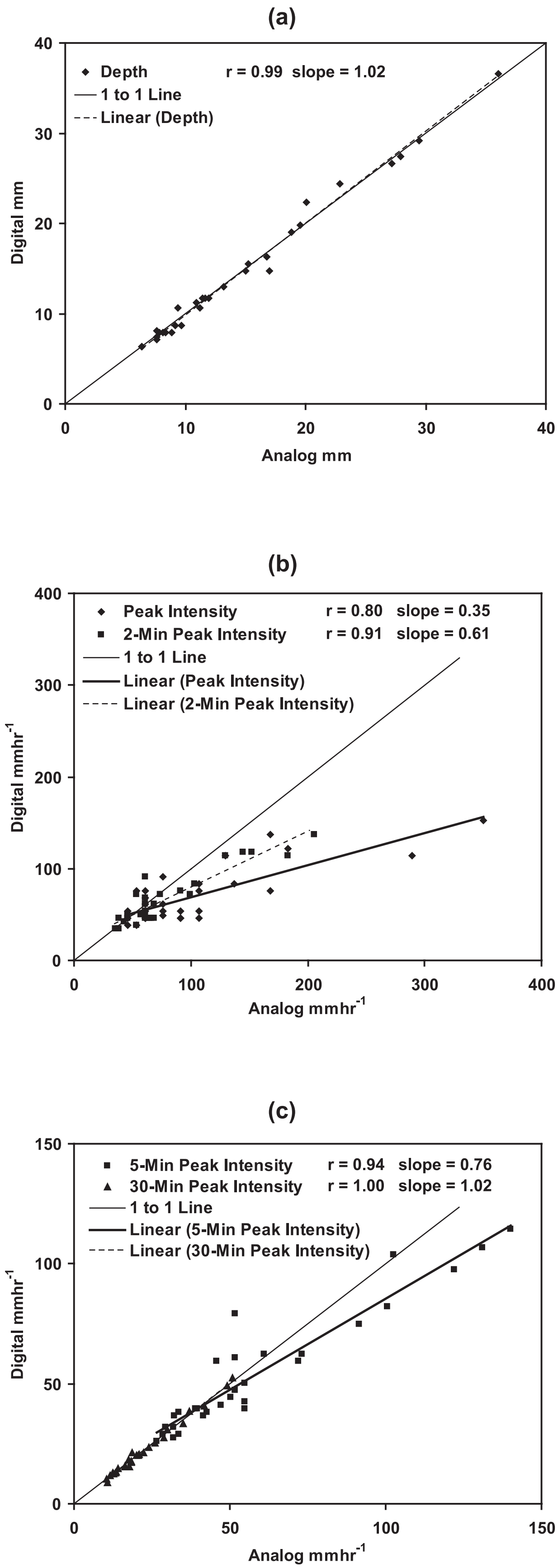


**Figure 11.** Correlation of 30 selected events for Kinematic and Erosion Runoff model (KINEROS) simulations. (a) Precipitation event depth. (b) Precipitation event peak and 2-min peak intensities. (c) Precipitation 5-min peak and 30-min peak intensities.

**Table 9.** Nash Sutcliffe Efficiency Statistic[a]

| Watershed | Runoff Volume | Runoff Duration | Runoff Peak Rate | Time to Peak Rate |
|---|---|---|---|---|
| 63.106 | 0.975 | 0.348 | 0.596 | 0.944 |
| 63.104 | 0.975 | 0.891 | 0.949 | 0.937 |

[a]Nash Sutcliffe Efficiency Statistic, E, for runoff simulation results for volume, duration, peak rate, and time to peak rate, as derived from digital and analog rain gauges for Lucky Hills watersheds 63.106 and 63.104.

models. For the analog and digital derived EI30 parameter, the high correlation (>0.99) and regression slopes within 10% of 1.00 indicated that the effect on RUSLE model simulations will be nil. Artificially high event peak rainfall intensities, as measured by the analog rain gauge at time intervals too short for accurate digitization, contributed to greater peak runoff rates at small watershed scales (<0.4 ha) using the KINEROS model. However, for an order-of-magnitude larger watershed (>4.0 ha), the effects of channels mitigated the differences in rainfall intensity peaks and temporal patterns, and model output differences were not significant.

[32] This multiyear multigauge comparison of a weighing bucket analog-recording rain gauge to its successor, a digital-recording electronic-weighing bucket rain gauge, was undertaken to establish quantifiable differences and similarities between the gauges during a period of coincident operation. This study provides a useful analysis for the WGEW and for other long-term rain gauge networks that have recently converted, or will soon convert, from analog to digital technology. Understanding these differences and similarities will benefit interpretation of the ultimately combined long-term precipitation record and provide insights into the impacts on hydrologic modeling.

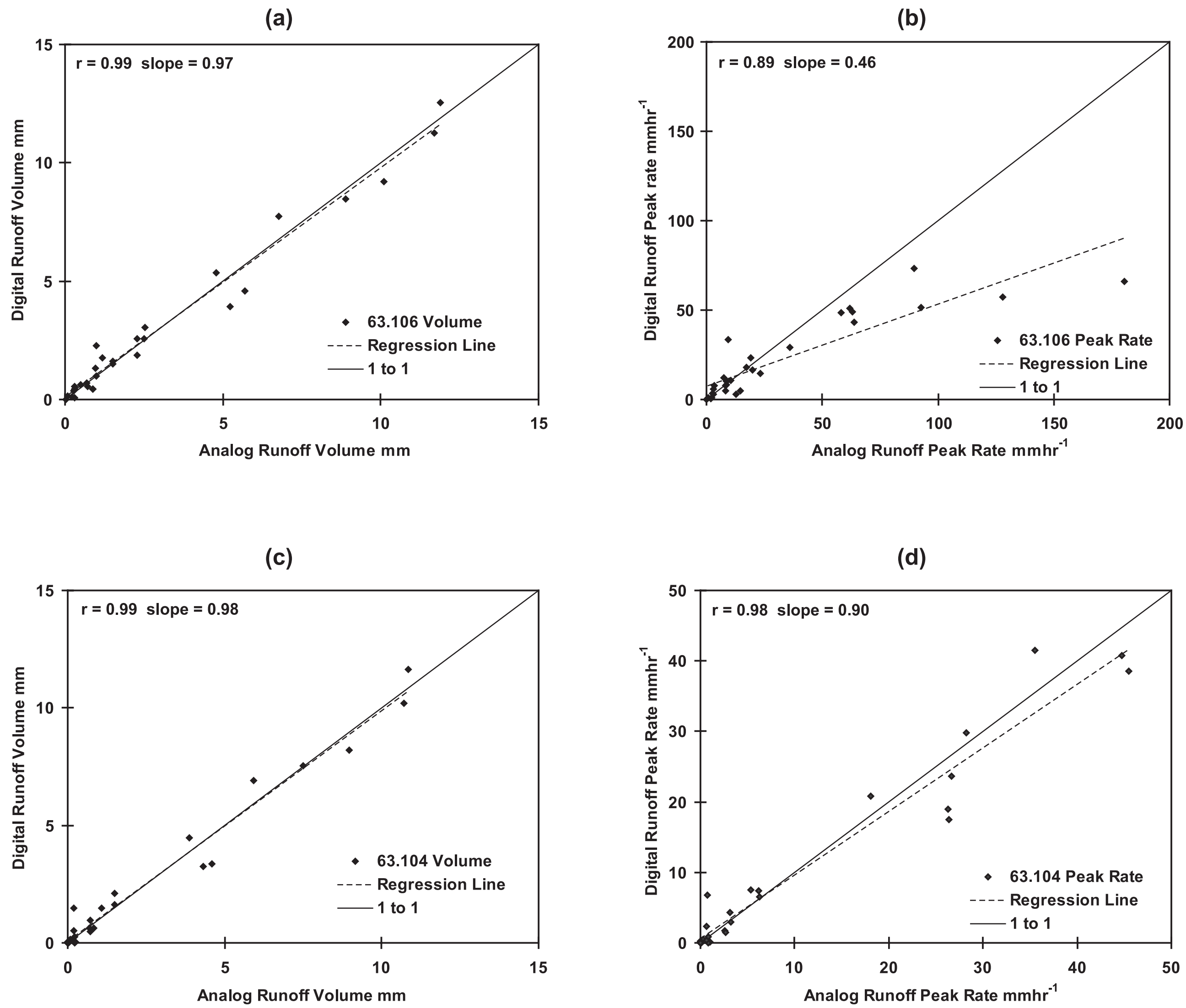


**Figure 12.** Correlation of 30 selected event runoff results for KINEROS simulations: (a) 63.106 event runoff volumes, (b) 63.106 event runoff peak rates, (c) 63.104 event runoff volumes, and (d) 63.104 event runoff peak rates.

[33] **Acknowledgments.** Special thanks to Rudy Ortiz, Jeff Kennedy, Lainie Levick, and all current and past SWRC workers who have contributed to the long-term collection, processing, and archiving of WGEW precipitation data, and in doing so have made this a preeminent database of semiarid precipitation.

## References

Bonta, J. V., L. B. Owens, and M. J. Shipitalo (2007), Watershed research at the North Appalachian Experimental Watershed at Coshocton, Ohio, in *Environmental and Water Resources Milestones in Engineering History*, edited by J. J. Rogers, pp. 127–134, ASCE/EWRI, Reston, Va.

Brakensiek, D. L., H. B. Osborn, and W. J. Rawls (Coord.) (1979), *Field Manual For Research In Agricultural Hydrology*, *Agric. Handb. 224*, 550 pp., U.S. Dept. of Agric., Washington, D. C.

Faures, J.-M., D. C. Goodrich, D. A. Woolhiser, and S. Sorooshian (1995), Impact of small-scale spatial rainfall variability on runoff modeling, *J. Hydrol.*, *173*, 309–326, doi:10.1016/0022-1694(95)02704-S.

Goodrich, D. C. (1990), *Basin Scale and Runoff Model Complexity*, *Tech. Rep. HWR 91-010*, 361 pp., Tech. Rep. on Nat. Resour. Syst., Univ. of Ariz., Tucson.

Goodrich, D. C., L. J. Lane, R. M. Shillito, S. N. Miller, K. H. Syed, and D. A. Woolhiser (1997), Linearity of basin response as a function of scale in a semiarid watershed, *Water Resour. Res.*, *33*(12), 2951–2965, doi:10.1029/97WR01422.

Goodrich, D. C., D. G. Williams, C. L. Unkrich, J. F. Hogan, R. L. Scott, K. R. Hultine, D. Pool, A. L. Coes, and S. Miller (2004), Comparison of methods to estimate ephemeral channel recharge, Walnut Gulch, San Pedro River Basin, Arizona, in *Groundwater Recharge in a Desert Environment: The Southwestern United States*, *Water Sci. Appl. Ser.*, vol. 9, edited by J. F. Hogan, F. M. Phillips, and B. R. Scanlon, pp. 77–99, AGU, Washington, D. C.

Goodrich, D. C., T. O. Keefer, C. L. Unkrich, M. H. Nichols, H. B. Osborn, J. J. Stone, and J. R. Smith (2008), Long-term precipitation database, Walnut Gulch Experimental Watershed, Arizona, United States, *Water Resour. Res.*, doi:10.1029/2006WR005782, in press.

Hanson, C. L. (2001), Long-term precipitation database, Reynolds Creek Experimental Watershed, Idaho, United States, *Water Resour. Res.*, *37*(11), 2831–2834, doi:10.1029/2001WR000415.

Hanson, C. L., M. D. Burgess, J. D. Windom, and R. J. Hartzmann (2001), New weighing mechanism for precipitation gauges, *J. Hydrol. Eng.*, *6*(1), 75–77, doi:10.1061/(ASCE)1084-0699(2001)6:1(75).

Harmel, R. D., K. W. King, C. W. Richardson, and J. R. Williams (2003), Long-term precipitation analyses for the Central Texas Blackland Prairie, *Trans. ASAE*, *46*(5), 1381–1388.

Keppel, R. V., and K. G. Renard (1962), Transmission losses in ephemeral streambeds, *J. Hydraul. Div. Am. Soc. Civ. Eng.*, *88*, 59–68.

Nash, J. E., and J. V. Sutcliffe (1970), River flow forecasting through conceptual models: I. A discussion of principles, *J. Hydrol.*, *10*, 282–290, doi:10.1016/0022-1694(70)90255-6.

National Research Council (1991), *Opportunities in the Hydrologic Sciences*, 368 pp., Natl. Acad. Press, Washington, D. C.

Nichols, M. H., and E. Anson (2008), Southwest Watershed Research Center Data Access Project, *Water Resour. Res.*, *44*, W05S03, doi:10.1029/2006WR005665.

Osborn, H. B., and L. Lane (1969), Prediction-runoff relation for very small semiarid rangeland watersheds, *Water Resour. Res.*, *5*(2), 419–425, doi:10.1029/WR005i002p00419.

Renard, K. G., and V. A. Ferreira (1993), RUSLE model description and database sensitivity, *J. Environ. Qual.*, *22*, 458–466.

Renard, K. G., and H. B. Osborn (1966), Rainfall intensity comparisons from adjacent 6-hour and 24-hour recording rain gages, *Water Resour. Res.*, *2*(1), 145–146, doi:10.1029/WR002i001p00145.

Renard, K. G., G. R. Foster, G. A. Weesies, D. K. McCool, and D. C. Yoder (Coord.) (1997), *Predicting Soil Erosion by Water: A Guide to Conservation Planning With the Revised Universal Soil Loss Equation (RUSLE)*, *Agric. Handb. 703*, 404 pp., U.S. Dept. of Agric., Washington, D. C.

Renard, K., M. Nichols, D. Woolhiser, and H. Osborn (2008), A brief background on the USDA-Agricultural Research Service: Walnut Gulch Experimental Watershed, *Water Resour. Res.*, doi:10.1029/2006WR005691, in press.

Smith, R. E., D. C. Goodrich, D. A. Woolhiser, and C. L. Unkrich (1995), KINEROS: A kinematic runoff and erosion model, in *Computer Models of Watershed Hydrology*, edited by V. P. Singh, pp. 697–732, Water Resour. Publ., Colo.

Stone, J. J., M. H. Nichols, D. C. Goodrich, and J. Buono (2008), Long-term runoff database, Walnut Gulch Experimental Watershed, Arizona, United States, *Water Resour. Res.*, *44*, W05S05, doi:10.1029/2006WR005733.

Syed, K. H., D. C. Goodrich, D. E. Myers, and S. Sorooshian (2003), Spatial characteristics of thunderstorm rainfall fields and their relation to runoff, *J. Hydrol.*, *271*(1–4), 1–21, doi:10.1016/S0022-1694(02)00311-6.

D. C. Goodrich, T. O. Keefer, M. S. Moran, J. R. Simanton, J. R. Smith, and C. L. Unkrich, Southwest Watershed Research Center, Agricultural Research Service, U.S. Department of Agriculture, Tucson, AZ 85719, USA. (tim.keefer@ars.usda.gov)